EUMETSAT Satellite Application Facility on Climate Monitoring

Visiting Scientist Report

Cloud2Power: Integrating Sunshine Duration from Ground and Satellite Observations for Agro-Energy Planning in Ghana

SAF_CM_DWD_VS25_01

By

Dr. Prince Junior Asilevi

Kwame Nkrumah University of Science and Technology, Kumasi, Ghana

Reference Number:	SAF/CM/DWD/CDOP4/VS25_01
Issue/Revision Index:	1.0
Date:	20.05.2026

Document Signature Table

	Name	Function	Signature	Date
Prepared by	Dr. Prince Junior Asilevi	Visiting Scientist		21. 01. 2026
Reviewed by	Marc Schröder	CM SAF Science Coordinator		20.05.2026
Approved by	CM SAF Steering Group			
Released by	Rainer Hollmann	CM SAF Project Manager		

Distribution List

Internal Distribution	
Name	No. Copies
DWD archive	1

External Distribution		
Company/Institute	Name	No. Copies
--	--	0

x Non-public document

◯ Public document

Document Change Record

Issue/ Revision	Date	Reason for changes	Changed Pages/Paragraphs
1.0	20.05.2026	First version	--

Table of content

List of Figures

List of Tables

1 Introduction

Sunshine duration (SD) is a fundamental indicator of near-surface radiative conditions and cloudiness (WMO, 2018). It provides an integrated measure of the combined effects of cloud cover, aerosol attenuation, and solar geometry, and has long been used in climatology, agrometeorology, hydrology, and renewable energy applications. Sunshine duration remains particularly relevant in regions where direct measurements of surface solar radiation are scarce, as it serves as a proxy for solar resource availability and atmospheric transmissivity (Asilevi et al., 2019; Wild, 2016; Wild 2009).

In sub-Saharan Africa, long-term ground-based observations of sunshine duration are limited in both spatial coverage and temporal continuity. Existing records are often affected by station relocations, changes in instrumentation (e.g., Campbell–Stokes recorders to automated sensors), observer practices, and data gaps, all of which complicate the detection of robust climate signals (Wild et al., 2013). These challenges are especially critical in the tropics, where cloud regimes are highly variable and where aerosols from biomass burning, mineral dust, and anthropogenic sources exert strong seasonal modulation on surface radiation (Bellouin et al., 2020). As a result, independent, spatially consistent climate data records (CDRs) are essential for assessing long-term variability and trends in sunshine duration across West Africa.
Satellite-derived CDRss offer a powerful complement to ground-based observations by providing spatially continuous and temporally homogeneous datasets over multi-decadal periods. The EUMETSAT Satellite Application Facility on Climate Monitoring (CM SAF) has developed a suite of CDRs for surface radiation based on geostationary satellite observations, among which the SARAH (Surface Solar Radiation Data Set – Heliosat) family is one of the most widely used (Pfeifroth et al., 2024; Hollmann et al., 2006). SARAH products employ the Heliosat method to retrieve surface shortwave radiation and sunshine duration from satellite-derived cloud properties, with inter-satellite calibration to ensure long-term consistency (Pfeifroth et al., 2023).

The most recent release, SARAH-3, represents a major advancement over earlier versions by extending temporal coverage back to 1983, i.e., more than 4 decades of data on a 0.05° x 0.05° spatial longitude/latitude grid (Pfeifroth et al., 2024), improving cloud detection and classification, refining radiative transfer parameterizations, and enhancing consistency across successive Meteosat generations. SARAH-3 provides daily, monthly, and climatological SD fields at high spatial resolution, making it highly attractive for climate monitoring, solar energy assessment, and trend analysis, particularly in data-sparse regions such as Africa.

However, the performance of satellite-derived SD products in tropical environments remains insufficiently documented. Tropical West Africa is characterized by complex and seasonally evolving cloud systems associated with the West African Monsoon, including deep convection, low-level stratiform clouds, and extensive mesoscale convective systems (Asilevi Junior et al., 2022; Knippertz et al., 2017). In addition, aerosol loading exhibits pronounced seasonality, with mineral dust outbreaks during the dry Harmattan season and widespread biomass-burning aerosols during boreal winter, both of which can significantly attenuate direct solar radiation without necessarily producing optically thick clouds (Clauzel et al., 2025; Dogbey et al., 2022). These conditions pose particular challenges for satellite algorithms that rely on cloud masking and parameterized clear-sky radiative transfer, potentially leading to systematic biases in sunshine duration estimates.

In particular, Ghana in West Africa provides an excellent laboratory for evaluating SARAH-3 performance under such conditions. Despite its relatively small geographic extent, the country spans multiple distinct climate zones, including the coastal savannah, forest, transitional, and northern savannah regions. These zones exhibit significant gradients in cloudiness, aerosol influence, and seasonal radiation regimes, ranging from persistent low-level cloud decks along the Gulf of Guinea coast to pronounced dry-season aerosol loading in the north (Asilevi Junior et al., 2022; Dogbey et al., 2022). The availability of long-term sunshine duration observations from the Ghana Meteorological Agency (GMet) further enables a station-based evaluation of satellite estimates.

Previous studies have demonstrated the value of SARAH products for solar radiation assessment in Europe and parts of Africa, but SD evaluations particularly focusing on bias characteristics, seasonal dependence, and trend consistency, remain limited over West Africa (Pfeifroth et al., 2024). Moreover, the potential role of aerosols in modulating satellite-ground SD discrepancies has received little attention, despite growing evidence of strong aerosol–radiation interactions in the region (Bellouin et al., 2020; Pinker et al., 2010).

Against this background, the current visiting scientist project sets out to deliver an evaluation of CM SAF SARAH-3 sunshine duration over Ghana for the period 1990–2024. By systematically comparing satellite estimates with observations from GMet, the analysis addresses climatological patterns, long-term trends, and bias characteristics across multiple spatial and temporal scales. Particular emphasis is placed on seasonal contrasts, dry-season aerosol influences, and conditions under which SARAH-3 may fail to capture very low sunshine duration (cloudy) days observed at the surface. Through this work, we aim to strengthen confidence in the use of SARAH-3 SD for climate monitoring and solar energy applications in West Africa, while also identifying limitations and pathways for future algorithm development.

To this end, the specific objectives of this study were to:

i. Characterize the spatial and seasonal SD climatology over Ghana using SARAH-3 and GMet observations;
ii. Quantify long-term trends in SD at station, zonal, and national scales;
iii. Assess systematic biases between SARAH-3 and GMet SD record and their seasonal dependence;
iv. Investigate aerosol controls on the SD bias; and
v. Identify meteorological conditions under which SARAH-3 fails to detect low-sunshine (cloudy) days.

2 Study Region, Data and Methods

2.1 Study Region

Ghana is located in the West Africa region between approximately 4.5°–11.5° N latitude and 3.5° W–1.5° E longitude and spans a significant south–north climatic gradient. The region lies entirely within the tropical belt and is strongly influenced by the seasonal migration of the Intertropical Discontinuity (ITD), that governs rainfall patterns, cloud cover, aerosol transport, and surface radiative conditions. As the ITD shifts northward and southward during the annual cycle, Ghana experiences marked seasonal contrasts in cloudiness and sunshine duration that are characteristic of the West African Monsoon system (Asilevi Junior et al., 2022; Dogbey et al., 2022). Figure 2-1 shows the radiation and sunshine potential of the area relative to the Meteosat full disk domain.

Climatologically, the area can be divided into four zones that differ substantially in cloud regime, atmospheric composition, and surface radiation (see Figure 2-2a). The coastal savannah zone along the Gulf of Guinea is influenced by maritime air masses and is characterized by frequent low-level stratiform cloud decks, particularly during the boreal summer monsoon season. Inland, the forest zone experiences persistent convective activity and high cloud fractions, leading to reduced sunshine duration during most of the year (see Figure 2-1). The transitional zone represents a climatic gradient between forest and savannah conditions, while the northern savannah zone is dominated by a unimodal rainy season and a prolonged dry season characterized by Harmattan winds and elevated mineral dust loading (Asilevi Junior et al., 2022; Knippertz et al., 2017). These contrasting regimes produce spatial and seasonal gradients in sunshine duration across Ghana and present a challenging environment for satellite-based retrievals.

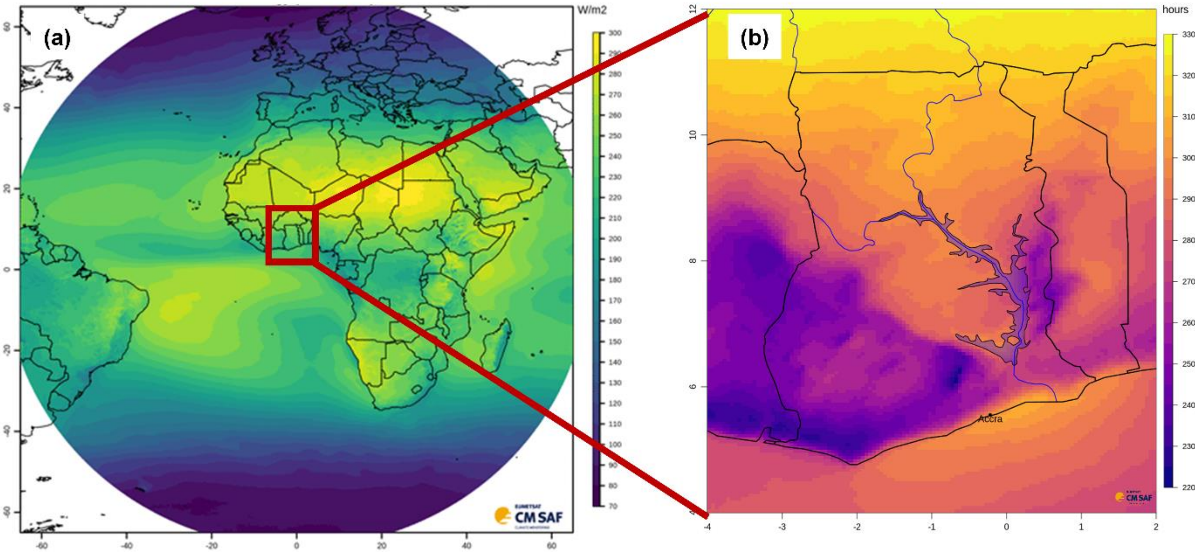

Figure 2-1: Study map showing the SARAH-3 long-term mean (a) global surface irradiance in units of W/m^2 and (b) sunshine duration in hours over Ghana during 1991 - 2020. Adapted from Pfeifroth et al. (2024).

2.2 Ground-Based Sunshine Duration Observations

Ground-based sunshine duration observations were obtained from the Ghana Meteorological Agency (GMet), which operates a national network of synoptic stations. The measurements were taken using the Campbell-Stokes Sunshine Recorder (CSSR) shown in Figure 2-2b, mounted at the 22 weather stations in Figure 2-2a, under unshaded conditions to ensure optimum sunlight exposure. The CSSR concentrates sunlight onto a thin strip of sunshine card (see Figure 2-1), which causes a burnt line representing the total period in hours during which sunshine intensity exceeds 120.0 Wm^{-2} according to World Meteorological Organization (WMO) standards, with hourly divisions on the card to determine the sunshine duration at an estimated resolution of 0.1 hour (Sánchez-Romero et al., 2015).

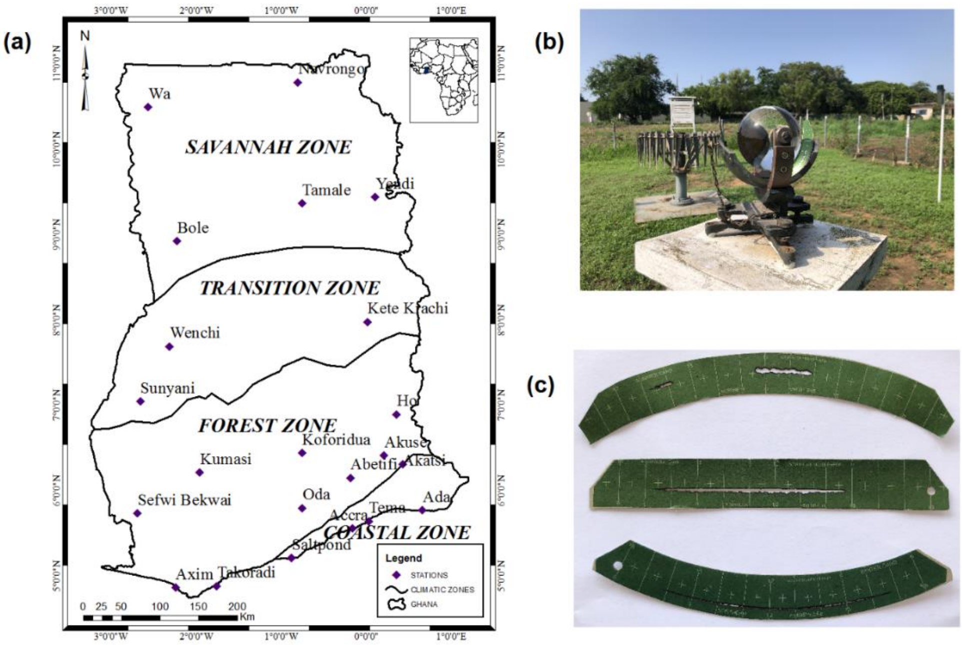

Figure 2-2: (a) Geopolitical map of the study area showing locations of the twenty-two (22) synoptic weather stations distributed countrywide, (b) the Campbell-Stokes Sunshine Recorder (CSSR) mounted at the 22 stations, and (c) the CSSR sunshine cards, each showing a burnt line indicative of sunshine duration in hours for particular days.

In principle, sunshine duration for a given day can be expressed as

$$\mathrm{SD} = \sum_{i=1}^{N_{obs}} \Delta t_i \ \text{ for } I_{b,i} \geq I_{thr} \qquad (1)$$

where $I_{b,i}$ is the direct normal irradiance during time interval Δt_i, I_{thr} is the sunshine threshold, and N_{obs} represents the number of observation intervals within the day. Although ground-based observations provide a direct and physically meaningful measurement of sunshine duration, they are subject to several limitations. These include spatial sparsity, data gaps, station relocations, changes in instrumentation, and observer-related uncertainties (Manara et al., 2015; Sánchez-Lorenzo et al., 2015).

2.3 CM SAF SARAH-3 Sunshine Duration Product

The Surface Solar Radiation Data Set – Heliosat (SARAH-3) is a satellite-based climate data record (CDR) developed by the EUMETSAT Satellite Application Facility on Climate Monitoring (CM SAF). SARAH-3 is doi-referenced (https://doi.org/10.5676/EUM_SAF_CM/SARAH/V003) and provides spatially and temporally consistent estimates of surface solar radiation and sunshine duration derived from geostationary Meteosat observations, with a temporal coverage extending from 1983 to the present.

Sunshine duration in SARAH-3 is retrieved indirectly using the Heliosat methodology, that combines satellite-derived cloud index information with clear-sky radiative transfer modelling. The cloud index quantifies the attenuation of surface solar radiation due to clouds relative to clear-sky conditions, while the clear-sky model accounts for solar geometry and atmospheric transmittance. A given time step is classified as “sunny” when the estimated surface direct irradiance exceeds the conventional sunshine threshold of 120 W m^{-2} (Pfeifroth et al., 2024).

The SD was derived from the ratio of the number of “sunny” satellite slots to all available slots during daylight multiplied by the theoretically possible daylength:

$$\mathrm{SD} = \mathrm{daylength} \cdot \frac{\sum_{i=1}^{iday}\left[W_i\left(\mathrm{sunny}_{\mathrm{slot}_i}\right)\right]}{\#\mathrm{daylight\_slots}} \qquad (2)$$

where W_i indicates the weighting of sunny slots depending on the number of surrounding cloudy and sunny grid points, and #daylight_slots is the number of daylight slots being the maximum number of Meteosat observations (slots) per grid point. The daily SDU is only calculated if at least 25 % of the possible daylight slots are available (Pfeifroth et al., 2024; Kothe et al., 2017).

2.4 Aerosol Data

To investigate aerosol potential controls on SD bias, daily aerosol optical depth (AOD) data were obtained from the Modern-Era Retrospective analysis for Research and Applications, Version 2 (MERRA-2). A long-term monthly mean SARAH AOD was juxtaposed with the MERRA-2 AOD to access AOD sensitivity. In principle, the AOD assimilates satellite aerosol retrievals, representing major aerosol species, including mineral dust, sea salt, black carbon, organic carbon, and sulfate aerosols (Randles et al., 2017).

2.5 Data Pre-processing and Quality Control

All datasets were harmonized to a common daily and monthly temporal framework covering the period 1990–2024, although the availability of valid paired observations varied between stations and periods following quality-control filtering. Quality control procedures were applied to both satellite and ground-based data to ensure physical consistency and comparability. These procedures included the removal of missing and flagged values, exclusion of non-physical sunshine duration values, and restriction of analyses to station-days with valid paired observations from both SARAH-3 and GMet. The as-received daily GMet and SARAH-3 SD records were quality controlled by ensuring $0 \leq n \leq N$, where N is the maximum or astronomical sunshine hours at the top of the atmosphere determined by Equation 2 by the site-specific latitude (ϕ) and solar declination (δ) computed by Equation 3 (Asilevi et. al., 2019):

$$N = \frac{2}{15}\cos^{-1}[-\tan\phi\tan\delta] \qquad (2)$$

$$\delta = 23.45\sin\left[360^{o} \times \frac{284 + J}{365}\right] \qquad (3)$$

where J represents the number for the Julian day of the year (first January is 1 and second January is 2).

Additional screening removed spurious values arising from observational or digitisation artefacts. Missing and placeholder values (−99 in GMet data) were removed and treated as invalid. To reduce the influence of non-meteorological artefacts, months with less than 20 days and mean SD below 1 h day^{-1} were excluded from climatological and trend analyses. Seasonal subsets were defined according to standard climatological conventions, with December - February representing the dry season, March - May the pre-monsoon transition, June - August the peak monsoon season, and September - November the post-monsoon transition. Zonal analyses were conducted by grouping stations according to their climatic zone and averaging across stations using only valid data.

2.6 Climatological Analysis

Climatological analyses were performed at daily, seasonal, and annual timescales. Daily climatologies were constructed by averaging sunshine duration for each day of the year across all available years, yielding a mean seasonal cycle that highlights recurring patterns in sunshine duration. Formally, the daily climatology can be expressed as:

$$\bar{SD}_{clim}(d) = \frac{1}{N_d}\sum_{y=1}^{N_d} SD(d, y) \qquad (4)$$

where d denotes the day of year, y represents the year, and N_d is the number of valid observations available.

2.7 Bias and Error Metrics

Sunshine duration bias was defined by Equation 5 as the difference between satellite-derived and ground-based observations.

$$\text{Bias} = SD_{SARAH} - SD_{GMet} \qquad (5)$$

Bias characteristics were quantified using the mean bias, absolute bias, and root-mean-square error. The RMSE provides a combined measure of systematic and random error and is defined by Equation 6.

$$\text{RMSE} = \sqrt{\frac{1}{N}\sum_{i=1}^{N}\left(SD_{sat,i} - SD_{obs,i}\right)^2} \qquad (6)$$

where N is the number of paired observations. Statistical relationships between datasets were further assessed using Pearson's correlation coefficient, which measures linear association, and Kendall's rank correlation coefficient, which captures monotonic relationships and is less sensitive to outliers.

2.8 Aerosol–SD Bias Relationship

To explore the role of aerosols in modulating SD bias, seasonal regression analyses were performed between SD bias and AOD bias. The relationship was expressed as

$$\mathrm{SD}_{\mathrm{bias}} = \gamma\,\mathrm{AOD}_{\mathrm{bias}} + \mathrm{c} \qquad (7)$$

where γ represents the sensitivity of SD bias to aerosol loading and c is a constant offset.

3 Results

3.1 Seasonal and Spatial Climatology of Sunshine Duration

The long-term seasonal climatology of SD derived from GMet observations and the CM SAF SARAH-3 dataset for 1990–2024 reveals a coherent seasonal cycle across all climate zones (Figure 3-1). Both datasets reproduce the expected modulation by the West African Monsoon system, with maximum sunshine duration during the boreal winter dry season (DJF), a marked decline during the onset and peak of monsoon activity (MAM–JJA), and partial recovery during the retreat phase (SON). This seasonal evolution is consistent with other climatologies of cloud cover, precipitable water, and atmospheric circulation over West Africa (Sawadogo et al., 2024; Knippertz et al., 2017).

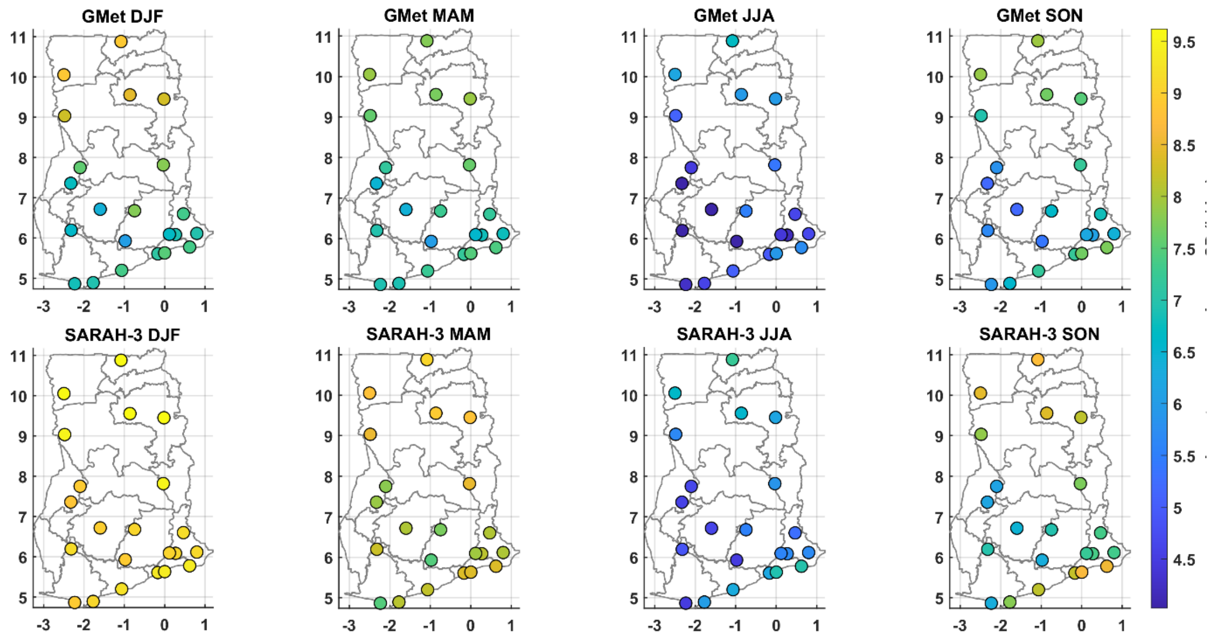

Figure 3-1: Comparison of long-term GMet and SARAH-3 seasonal mean SD (1990-2024).

Despite the consistent phasing, SARAH-3 systematically reports higher sunshine duration than GMet across all seasons and climate zones. The magnitude of this positive offset is spatially structured, with the largest discrepancies observed in the Forest and Coastal Savannah zones and comparatively smaller differences in the northern Savannah. This spatial pattern reflects the increasing prevalence of low-level stratiform cloud decks and maritime cloud systems toward southern Ghana, which are known to be challenging for satellite-based cloud detection and sunshine duration retrievals from geostationary platforms (Quansah et al., 2022; Adler et al., 2017; Schrage and Fink, 2012).

The long-term mean daily SD (Figure 3-2) further highlights this gradient. GMet observations indicate mean values ranging from approximately 6–7 h day^{-1} in the coastal and forest zones to 8–9 h day^{-1} in the northern savannah. SARAH-3 captures the broad north–south contrast but exhibits a uniform positive bias, particularly over the coastal belt. This behavior suggests that SARAH-3 may under-detect persistent cloudiness or partially cloudy conditions in regions dominated by shallow cumulus and stratocumulus, which exert a strong control on direct solar irradiance but may not always be classified as optically thick cloud in satellite algorithms (Holmlund et al., 2025; Pfeifroth et al., 2024).

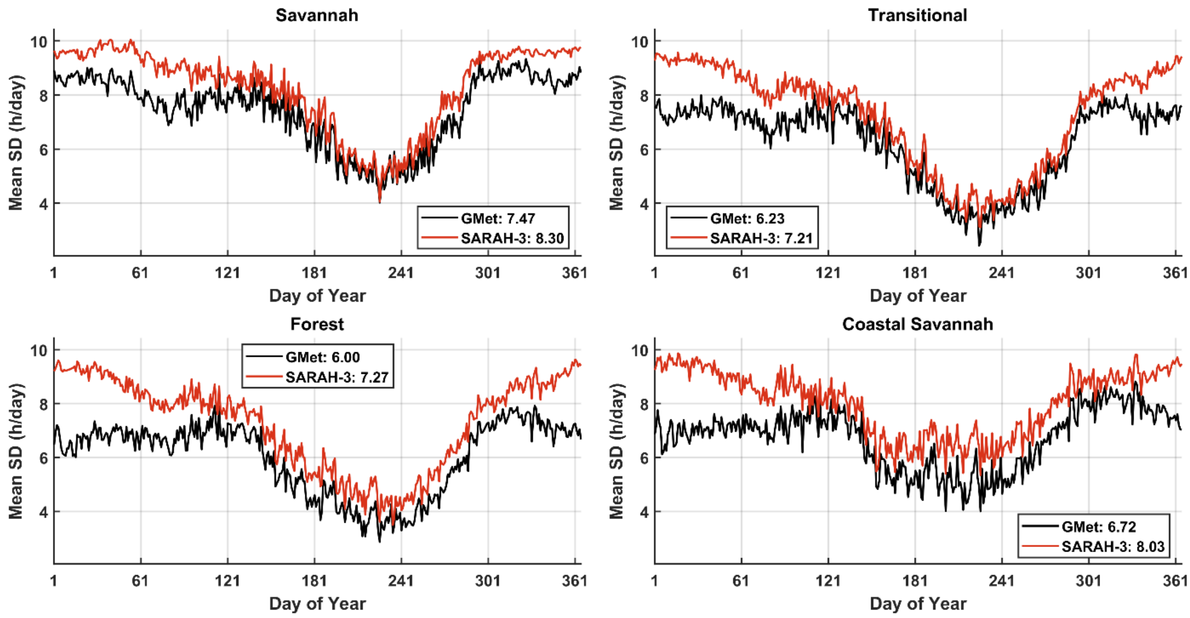

Figure 3-2: Mean annual cycle of zonal daily sunshine duration from GMet and SARAH-3 across the four climatic zones of Ghana.

3.2 SARAH-3 and GMet SD Bias Distribution and Characteristics

Beyond mean bias characteristics, the full distribution of SD biases in SARAH-3 against GMet reveals important season- and zone-dependent behaviour. The seasonal spatial distributions in Figure 3-3 indicate that DJF biases are not only larger but also spatially coherent, extending from the northern savannah into the coastal south. In contrast, JJA biases are smaller, spatially heterogeneous, and in some locations approach near-zero values.

This reduction in bias magnitude during JJA is consistent with the dominance of optically thick, vertically extensive cloud systems during the West African monsoon, which are more readily detected by geostationary satellite cloud masks (Karlsson et al., 2017). Under such conditions, both satellite and ground instruments agree more closely on the absence of direct sunshine.

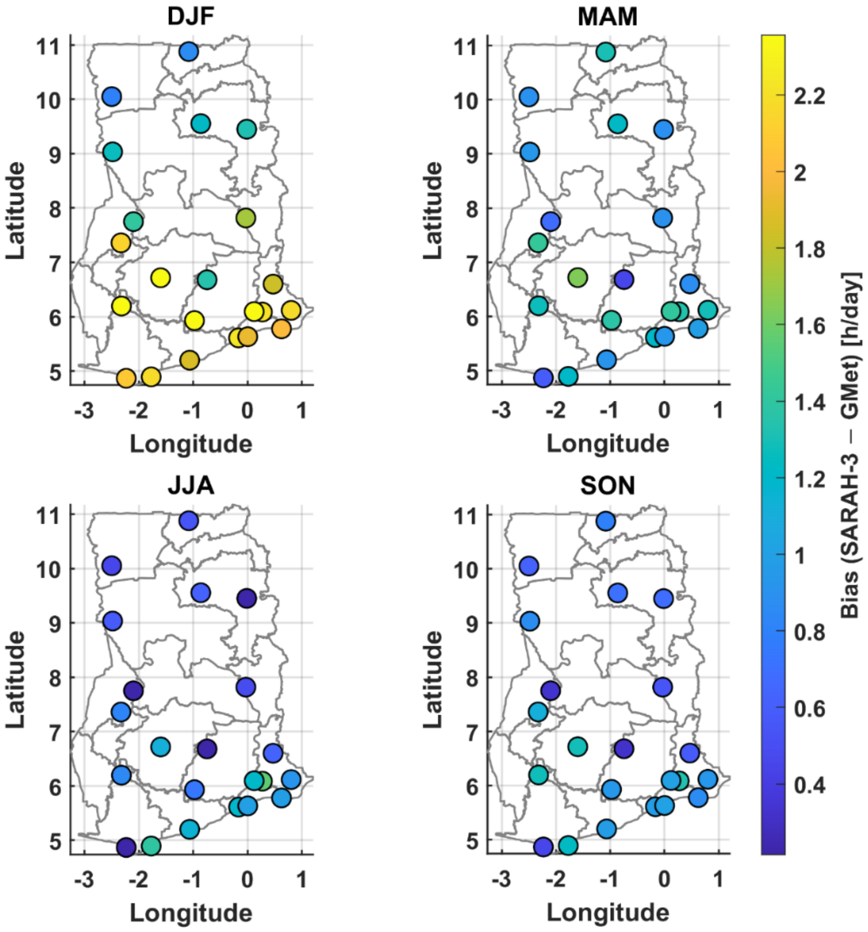

Figure 3-3: Seasonal comparison in the SARAH-3 and GMet SD bias.

The lower maximum biases observed during SON further suggest a gradual transition toward more stable retrieval conditions as aerosol loading decreases and cloud regimes shift toward stratiform and shallow convective types. These findings align with previous evaluations of CM SAF radiation products in tropical Africa, which report seasonally varying performance linked to cloud type and aerosol conditions. Table 3-1 summarizes the seasonal bias statistics derived from daily collocated station–satellite matchups. Mean biases range from 0.76 h day^{-1} in JJA to 1.86 h day^{-1} in DJF, with median biases closely tracking the means, indicating relatively symmetric bias distributions. The larger spread during DJF, as reflected by the higher standard deviation (0.56 h day^{-1}), points to enhanced variability in retrieval performance under dry-season aerosol conditions, when mineral dust and biomass-burning aerosols are prevalent over Ghana.

Table 3-1: Summary statistics for the GMet vs SARAH-3 SD bias for winter (DJF), spring (MAM), summer (JJA) and autumn (SON) daily collocated matchups.

Season	Mean Bias	Median Bias	Std Bias	Min Bias	Max Bias
DJF	1.86	1.96	0.56	0.79	2.81
MAM	1.08	1.10	0.30	0.45	1.64
JJA	0.76	0.78	0.42	0.00	1.56
SON	0.86	0.90	0.30	0.32	1.33

3.3 Long-term Trends in Sunshine Duration

The long-term evolution of sunshine duration was assessed. Figure 3-4 presents the spatial distribution of station-level trends from GMet and SARAH-3, while Figure 3-5 and Table 3-2 summarize the corresponding zonal-mean temporal evolution and trend magnitudes across the major climatic zones.

In general, GMet stations exhibit larger positive trend of +3.17 h decade^{-1} (Figure 3-4, left), whereas SARAH-3 trends are comparatively weaker and spatially smoother. However, these differences may be because valid temporal coverage differs between stations and between the two datasets after quality control filtering. Consequently, part of the observed trend differences may arise from differences in temporal sampling and data coverage rather than solely from physical inconsistencies between the datasets.

In contrast, SARAH-3 shows much weaker station-level trends, with a mean of +1.02 h decade^{-1} (Figure 3-4, right). The spatial pattern is notably smoother, with most stations exhibiting near-zero to weakly positive trends. This muted response relative to

GMet suggests that SARAH-3 captures the long-term mean state of surface solar conditions more conservatively, potentially reflecting the stabilizing influence of satellite retrieval homogenization and cloud detection thresholds embedded in the Heliosat framework (Pfeifroth et al., 2018).

The systematic reduction in trend amplitude in SARAH-3 relative to GMet may also indicate a partial attenuation of decadal variability linked to local cloud microphysics, low-level stratus, and aerosol–cloud interactions, which are challenging to resolve using geostationary visible-channel–based methods in humid tropical environments (Posselt et al., 2012; Karlsson et al., 2020).

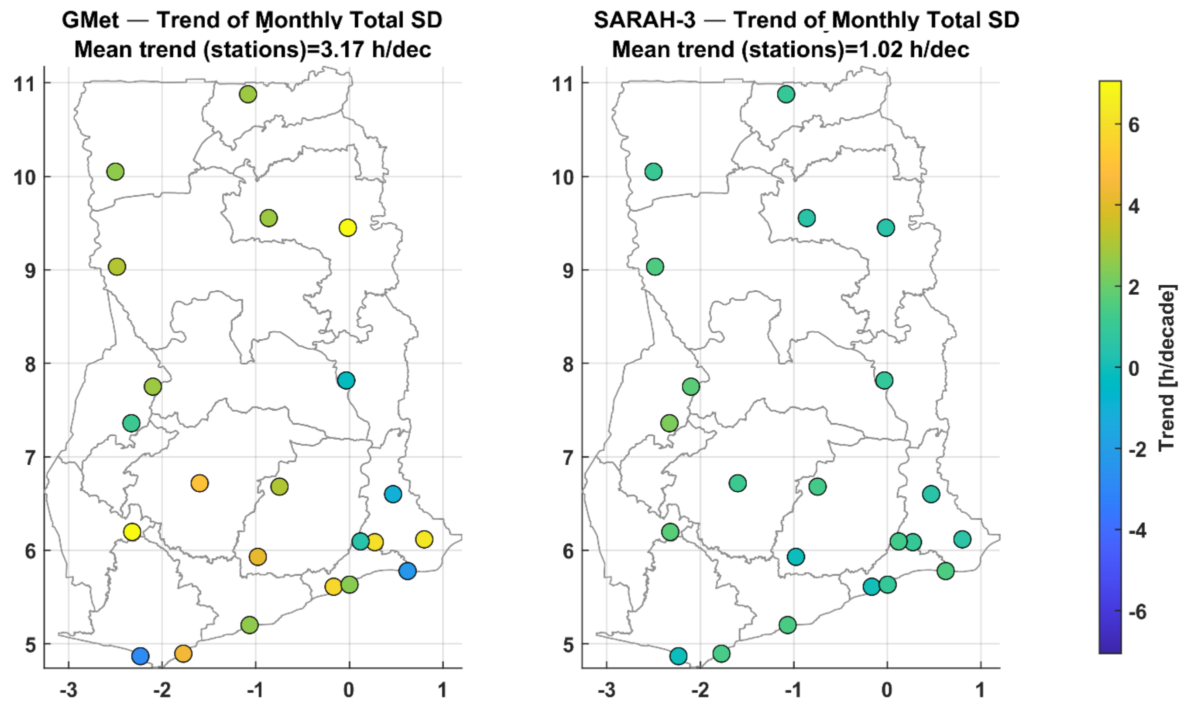

Figure 3-4: Station-level trends in monthly total sunshine duration (SD) for GMet and SARAH-3. Trends are computed using available valid monthly data within 1990–2024. Because valid temporal coverage differs between stations and between GMet and SARAH-3 after quality control filtering, the absolute trend magnitudes in the two datasets are not directly comparable.

The zonal-mean time series and SD bias (SARAH-3 − GMet) time series shown in Figure 3-5 and Figure 3-6 respectively provide further insight into the consistency and robustness of the trends. All four climatic zones exhibit pronounced seasonal cycles in monthly sunshine duration, with maxima during the dry season and minima during the monsoon months, consistent with established climatology over Ghana (Duku et al., 2011; Owusu & Waylen, 2013). Quantitatively, Table 3-2 shows that GMet zonal trends are positive in three out of four zones, ranging from 0.07 h decade^{-1} in the Savannah to 0.16 h decade^{-1} in the Forest zone, with a weak negative trend (−0.04 h decade^{-1}) in the Transitional zone. SARAH-3 trends are uniformly weaker, ranging between 0.01 and 0.03 h decade^{-1}, and show little zonal contrast.

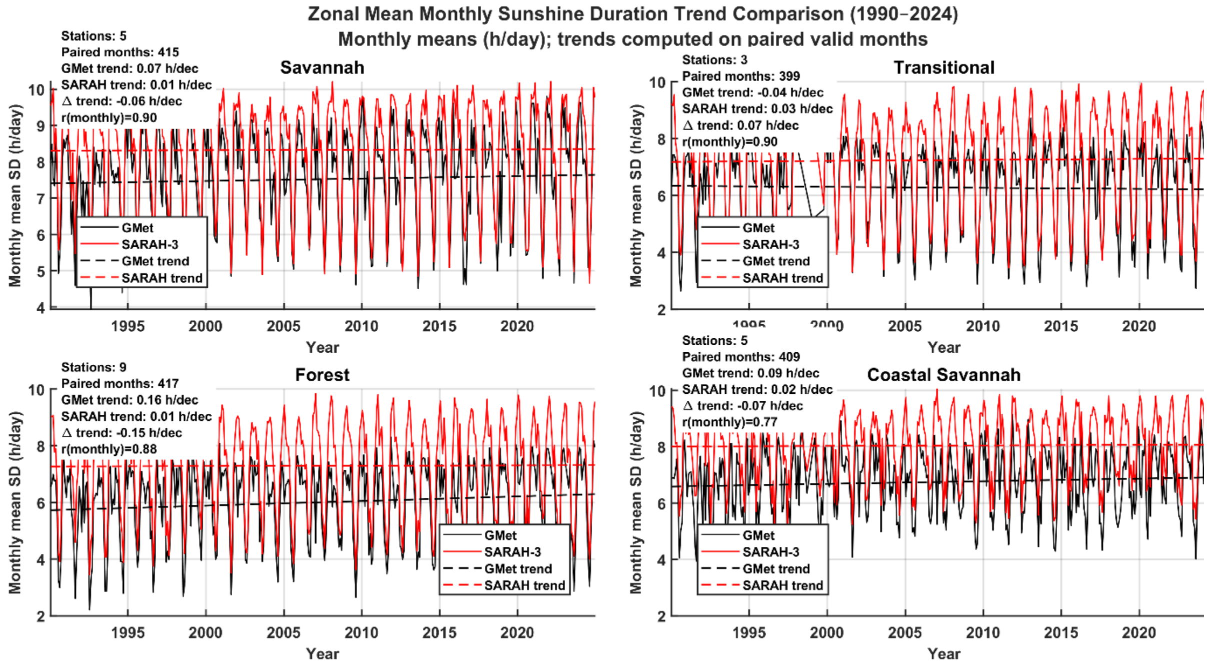

Figure 3-5: Long-term zonal mean trend comparison.

Table 3-2: Summary statistics of zonal mean SD trends.

	Slope (h/ dec)		Mean SD	
Zone	GMet	SARAH-3	GMet	SARAH-3
Savannah	0.07	0.01	7.52	8.33
Transitional	-0.04	0.03	6.27	7.24
Forest	0.16	0.01	6.01	7.29
Coastal Savannah	0.09	0.02	6.75	8.04

The largest discrepancy between datasets occurs in the Forest and Coastal Savannah zones, where GMet indicates stronger brightening than SARAH-3. These regions are characterized by persistent low- and mid-level cloudiness, frequent convective activity, and high aerosol loads from biomass burning and urban emissions, particularly during the dry season (Asilevi et al., 2025). Such conditions can enhance sensitivity to instrument type and observational method, potentially amplifying long-term trends in ground-based records relative to satellite-derived estimates.

From Figure 3-6, the SD bias (SARAH-3 − GMet) is predominantly positive in all zones, indicating systematic overestimation by SARAH-3 relative to ground observations. Interannual variability is evident, with larger fluctuations in the southern zones. The fitted linear trends are weak, suggesting that the satellite–ground discrepancy remains largely stable over the study period rather than exhibiting strong long-term divergence.

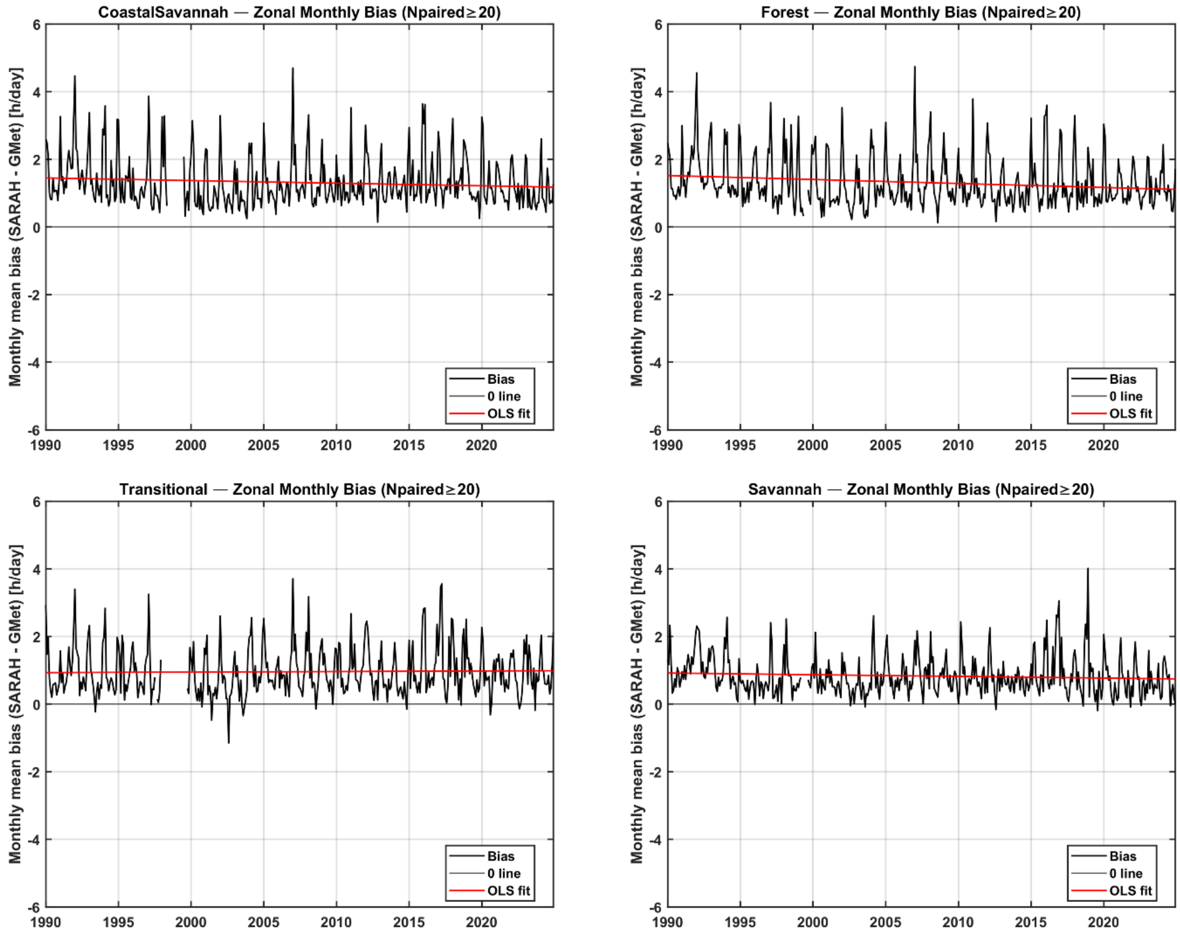

Figure 3-6: Zonal mean monthly SD bias (SARAH-3 − GMet) for the Coastal Savannah, Forest, Transitional, and Savannah zones (1990–2024).

3.4 Coupling Between Sunshine Duration Bias and Aerosol Optical Depth

To investigate whether aerosol loading contributes to the observed SARAH-3 SD bias, we analysed the relationship between SD bias (SARAH–GMet) and aerosol optical depth (AOD) bias (MERRA-2 minus SARAH) using paired daily observations over the common analysis period 1990–2024.

Figure 3-7 presents the seasonal spatial distribution of the Pearson correlation coefficient (r) between SD bias and AOD bias across Ghana, based on stations with at least 150 paired daily observations per season. A clear seasonal contrast emerges. During DJF, correlations are predominantly moderate to strong and positive across most stations, with a national mean r of 0.59. This indicates that days with higher positive AOD bias are generally associated with larger positive sunshine duration bias, suggesting that aerosol conditions play an important role in modulating satellite-derived sunshine estimates during the dry season.

In MAM, the correlation weakens (mean r = 0.41) but remains positive at most stations, particularly over the coastal and forest zones. This transitional season is characterized by increasing cloudiness and convective activity, which likely introduces competing cloud-related uncertainties that partially obscure the aerosol signal. By contrast, correlations during JJA are uniformly weak (mean r = 0.13), with several stations exhibiting near-zero or even slightly negative values. This reflects the dominance of thick monsoon cloud decks during the peak rainy season, when sunshine duration is primarily controlled by cloud cover rather than aerosol attenuation. In SON, correlations recover slightly (mean r = 0.20), consistent with the gradual re-emergence of aerosol influences as cloudiness decreases.

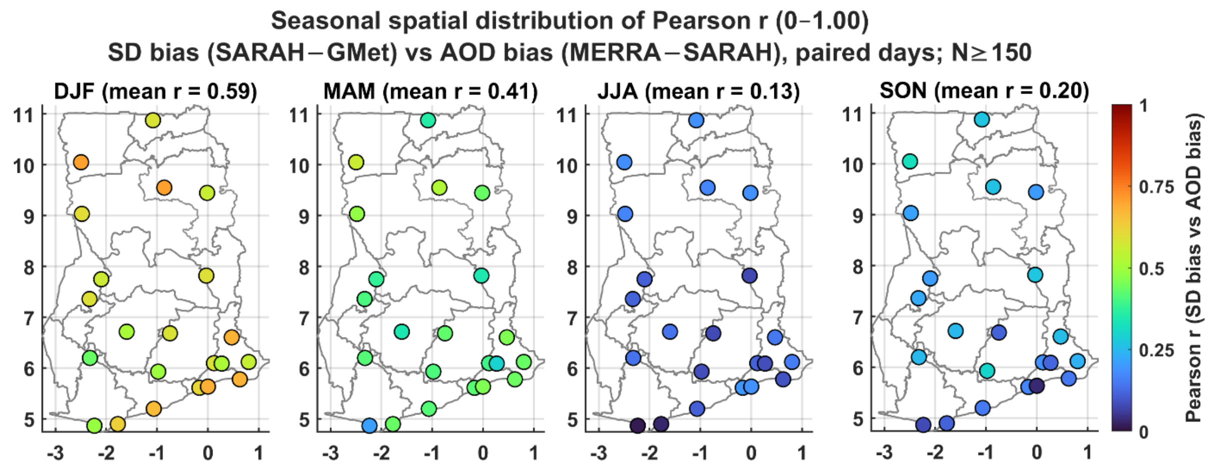

Figure 3-7: Spatial distribution of seasonal mean SD bias – AOD bias correlation.

These patterns demonstrate that aerosol–sunshine interactions are highly season-dependent, exerting the strongest influence during dry and pre-monsoon periods and becoming secondary during peak monsoon conditions.

The relationship is further quantified in Figure 3-8, which shows density-based scatter plots of daily SD bias against AOD bias for each season. The DJF exhibits a well-defined positive relationship, with a Pearson correlation and a regression slope of approximately 3.20 h day^{-1} per unit AOD bias. This steep slope implies that even modest positive AOD biases can translate into substantial overestimation of sunshine duration by SARAH-3 during the dry season.

In MAM, the slope decreases to about 2.19 h day^{-1} per unit AOD bias, and the correlation weakens (r = 0.39), consistent with increasing cloud variability. During JJA, both the correlation (r = 0.13) and slope (1.89 h day^{-1} per unit AOD bias) are markedly reduced, indicating that aerosol effects are largely masked by cloud-driven radiative extinction. SON shows intermediate behaviour, with a slope of 1.76 h day^{-1} per unit AOD bias and r = 0.18.

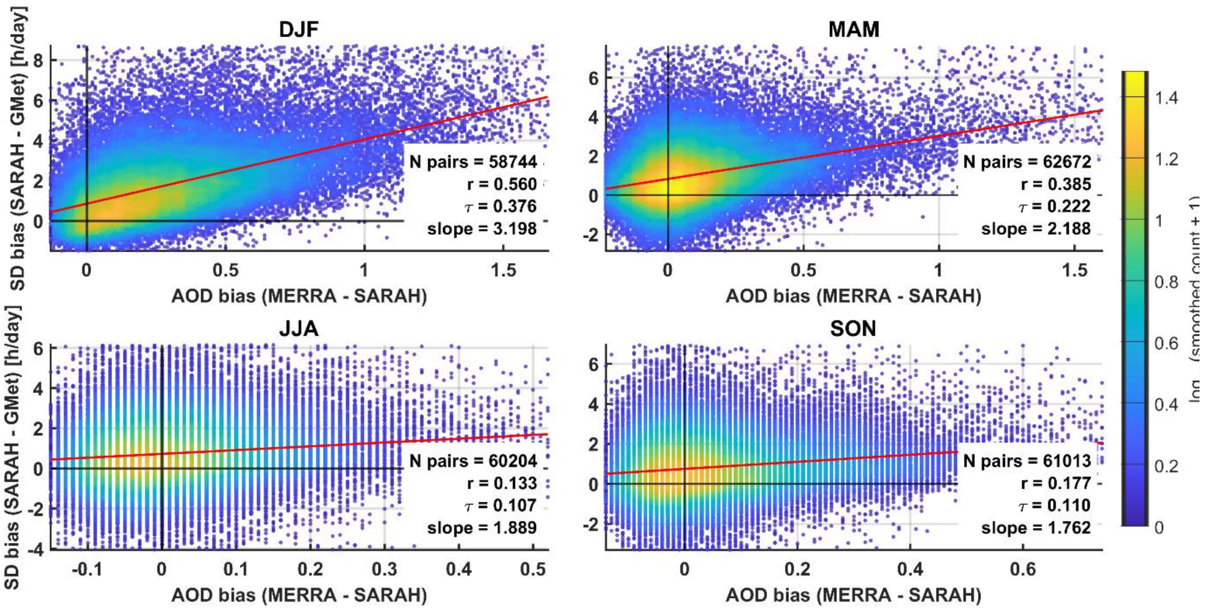

Figure 3-8: Comparison of seasonal SD bias and AOD bias in GMet and SARAH-3 datasets.

These results suggest that SARAH-3 SD retrievals are particularly sensitive to aerosol representation under clear-sky or broken-cloud conditions, but much less so under persistent overcast regimes.

Table 3-3 synthesizes the seasonal statistics of the SD bias–AOD bias relationship. DJF exhibits the largest mean SD bias (1.85 h day^{-1}), the highest correlation with AOD bias (r = 0.56), and the largest regression slope, alongside elevated RMSE values for both SD and AOD bias. This combination highlights DJF as the season in which aerosol-related uncertainties exert the strongest influence on SARAH-3 performance over Ghana.

In contrast, JJA shows the smallest mean SD bias (0.77 h day^{-1}), minimal AOD bias (0.02), and the lowest RMSE, reinforcing the conclusion that cloud processes dominate sunshine duration variability during the monsoon season. MAM and SON occupy intermediate positions, reflecting mixed aerosol–cloud control regimes.

Table 3-3: Summary statistics of seasonal SARAH-3 and GMet SD bias.

Season	Pearson (r)	Slope (h day^{-1})	Mean SD Bias (h day^{-1})	Mean AOD Bias	RMSE SD Bias (h day^{-1})	RMSE AOD Bias
DJF	0.56	3.20	1.85	0.31	2.61	0.45
MAM	0.39	2.19	1.09	0.12	1.92	0.30
JJA	0.13	1.89	0.77	0.02	1.76	0.11
SON	0.18	1.76	0.86	0.06	1.74	0.16

Further, Figure 3-9 maps the spatial distribution of regression slopes between SD bias and AOD bias, providing insight into regional sensitivity. The largest slopes during DJF are observed over the coastal savannah and southern forest zones, where dry season biomass burning plumes, urban pollution, and maritime aerosols frequently coexist. These regions also coincide with areas where SARAH-3 tends to overestimate sunshine duration relative to GMet observations. Northern savannah stations exhibit comparatively lower slopes, possibly caused by differences in aerosol type, vertical distribution, or surface albedo effects.

During JJA, regression slopes are uniformly low across all regions, reinforcing the weak coupling observed in the correlation analysis. The modest recovery of slopes in SON again highlights the transition back toward aerosol-sensitive conditions.

The observed coupling between sunshine duration bias and aerosol loading is physically consistent with the radiative principles underpinning the WMO sunshine duration definition, which relies on a direct solar irradiance threshold. Aerosols can attenuate direct solar radiation without necessarily producing optically thick clouds detectable by satellite cloud masks, leading to misclassification of marginal sunshine conditions. If aerosol absorption or scattering is underestimated in the retrieval chain, satellite products may overestimate sunshine duration, particularly under dry, hazy conditions.

These results suggest that improving aerosol characterization could substantially reduce sunshine duration biases in SARAH-type products over West Africa. The results also underscore the importance of seasonally stratified validation, as annual-mean performance metrics can obscure strong regime-dependent errors.

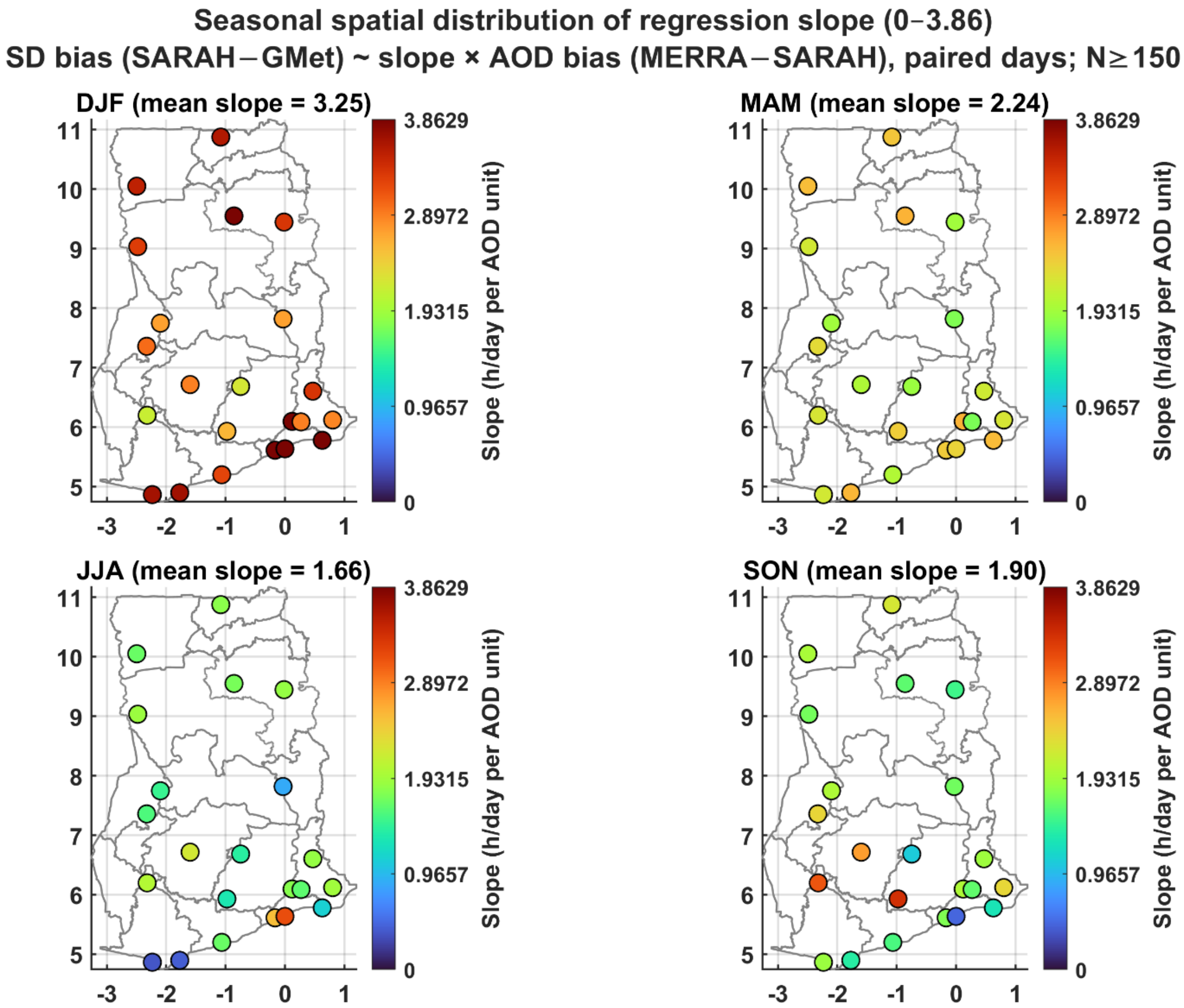

Figure 3-9: Station level spatial distribution of the SD bias and AOD bias slopes.

The relatively strong correlations observed during DJF and MAM suggest that MERRA-2 AOD captures aerosol variability that is dynamically linked to SD bias. This supports the suitability of MERRA-2 AOD as a diagnostic variable for understanding and potentially correcting SARAH-3 SD retrieval errors. Incorporating improved aerosol representation in future algorithm refinements may therefore enhance SD accuracy over West Africa.

3.5 Sunshine Duration Frequency Distribution

The frequency distribution analysis provides additional insight into the structural differences between SARAH-3 and GMet SD. Figure 3-10 presents the zonal frequency distributions of daily zonal SD over the full paired period (1990–2024). Across all zones, both datasets exhibit broadly similar unimodal distributions, with peaks shifting systematically from higher values in the northern Savannah to lower values in the Forest zone, reflecting the well-known latitudinal gradient in cloudiness and moisture availability over the region. This spatial consistency indicates that SARAH-3 successfully captures the large-scale climatic controls on sunshine duration.

However, important distributional differences emerge. In all zones, SARAH-3 distributions are systematically shifted toward higher sunshine duration values relative to GMet, as evidenced by higher zonal means and upper-percentile ranges. For example, in the Savannah zone, the mean SD is ~ 8.32 h day^{-1} in SARAH-3 compared to ~ 7.51 h day^{-1} in GMet, with the SARAH-3 P10 - P90 (10th and 90th percentiles) range extending further into high-sunshine conditions. Similar shifts to larger SD values are observed in the Transitional, Forest, and Coastal Savannah zones. This consistent displacement suggests a systematic positive bias in SARAH-3, particularly in moderate-to-high sunshine regimes.

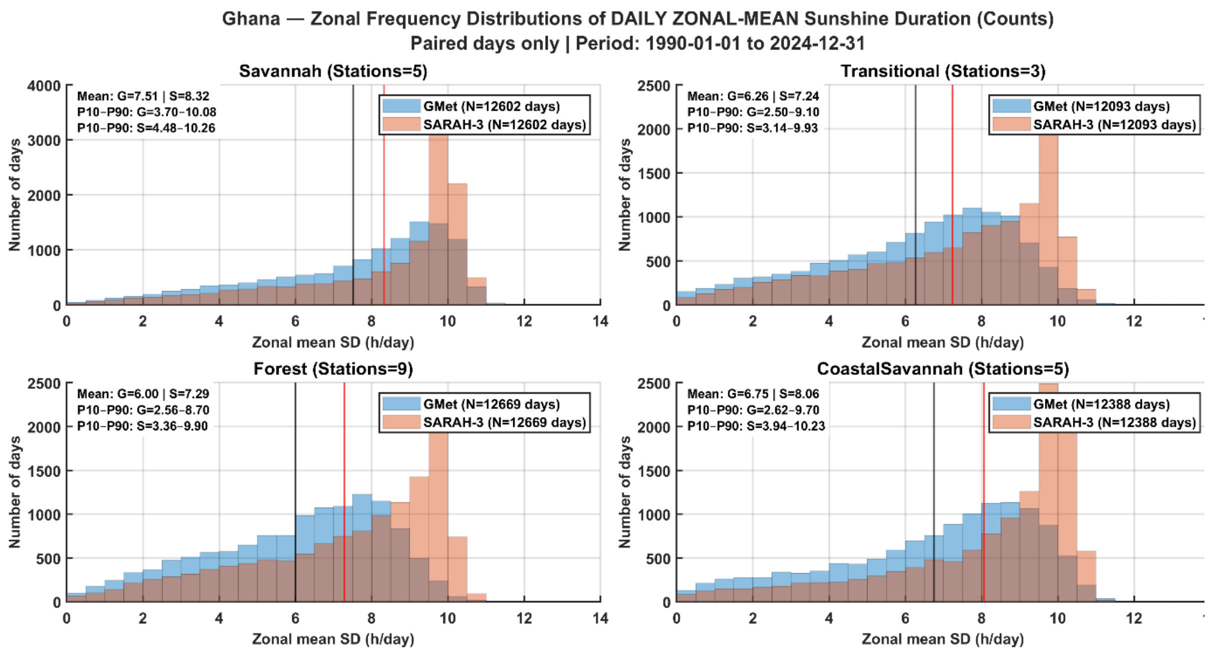

Figure 3-10: Zonal comparison of SARAH-3 and GMet SD frequency distribution. P10 - P90 is the 10th and 90th percentiles.

The lower tail of the distributions reveals another discrepancy. GMet exhibits a substantially higher frequency of low-sunshine days (below ~ 2 h day^{-1}) across all zones, especially in the Forest and Coastal Savannah regions, where persistent cloudiness associated with deep convection and maritime inflow is common. In contrast, SARAH-3 shows a compressed lower tail, with fewer occurrences of very low sunshine duration. This behavior is consistent with known challenges in satellite-based sunshine duration retrievals under optically thick cloud conditions, where partial cloud breaks, sub-pixel heterogeneity, and threshold-based sunshine definitions may lead to an overestimation of sunshine duration (Pfeifroth et al., 2018).

These distributional differences are further highlighted in Figure 3-11, which focuses explicitly on Coastal Savannah JJA days for which GMet reports SD below 1 h day^{-1}. Under these conditions, GMet measurements cluster tightly near zero, with a mean of 0.42 h day^{-1}, reflecting persistent low-level cloud cover, marine stratocumulus, and monsoon-related overcast conditions typical of the West African coastal zone during boreal summer. In contrast, SARAH-3 reports a markedly broader distribution, with a mean of 1.63 h day^{-1} and a substantial fraction of cases exceeding 1 h day^{-1} (61%), 2 h day^{-1} (31%), and even 4 h day^{-1} (6%).

This divergence provides strong evidence that SARAH-3 systematically overestimates SD during heavily overcast conditions. Physically, this behavior likely arises from a combination of factors. First, the Heliosat-based approach relies on cloud index and irradiance thresholds that may not fully resolve low-sun conditions associated with broken stratiform cloud decks or thin cloud layers common in coastal West Africa. Second, geostationary satellite retrievals may exhibit non-linear threshold effects under predominantly cloudy conditions, where small cloud gaps within overcast scenes intermittently elevate irradiance estimates above sunshine detection thresholds. Third, aerosol–cloud interactions, particularly during the monsoon season, may alter radiative properties in ways that challenge satellite cloud discrimination algorithms (Pfeifroth et al., 2024; Pfeifroth et al., 2018).

Importantly, the results in Figure 3-9 and Figure 3-10 complement the bias and aerosol-coupling analyses presented in Sections 3.2 and 3.4. The systematic underrepresentation of very low sunshine days in SARAH-3 helps explain the positive mean SD biases observed across all seasons and zones (Table 3-1) and the weaker bias–AOD coupling during JJA (Figure 3-6), when cloudiness dominates over aerosol radiative effects. Together, these findings suggest that while SARAH-3 performs robustly in representing spatial patterns, seasonal cycles, and long-term trends, caution is warranted when using the dataset to characterize extreme low-sunshine conditions, particularly in coastal and forested regions during the monsoon season.

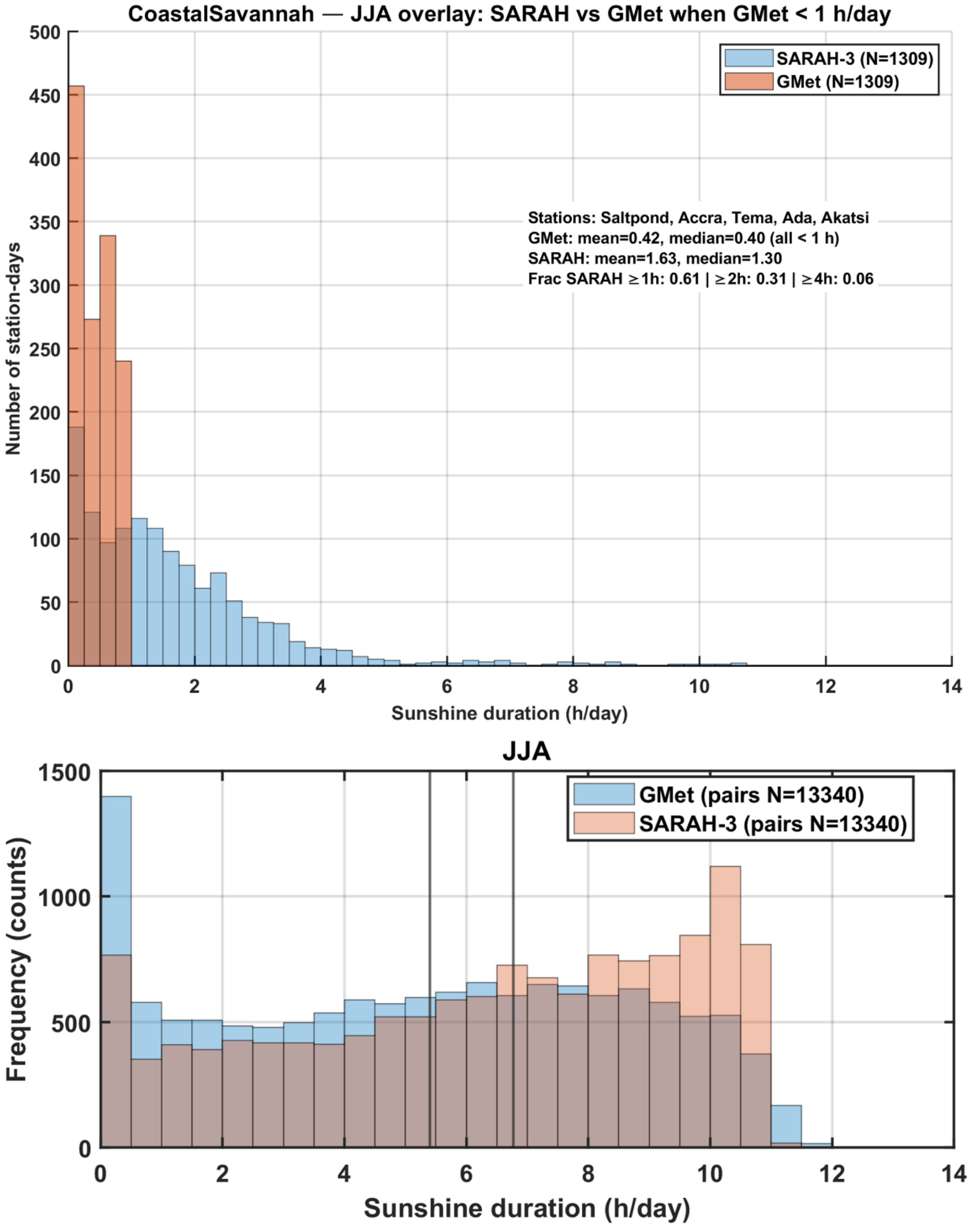

Figure 3-11: Frequency distribution over the Coastal Savannah zone in SARAH-3 SD when GMet SD < 1 hour (upper figure) and during the JJA season (lower figure).

4 Conclusions

This work aimed to develop a robust, multi-decadal evaluation of CM SAF SARAH-3 SD over Ghana in West Africa for the period 1990–2024, integrating ground-based observations from the Ghana Meteorological Agency (GMet) with satellite-derived climate data records. By combining climatological analysis, trend assessment, bias characterization, aerosol coupling, and distributional diagnostics across distinct climatic zones, the work provides both methodological validation and physical interpretation of SARAH-3 performance in a tropical West African context.

At the climatological scale, SARAH-3 successfully reproduces the broad spatial and seasonal patterns of SD across Ghana, capturing the north–south gradient associated with cloudiness, rainfall regimes, and aerosol loading. However, a systematic positive bias relative to GMet is evident in all seasons, with the largest magnitudes occurring during the dry Harmattan period (DJF) and the smallest during the peak monsoon season (JJA). These seasonal contrasts indicate that SARAH-3 performance is strongly modulated by prevailing atmospheric conditions rather than by static surface or orbital factors alone.

Long-term trend analysis reveals differences between ground-based and satellite-derived SD. In general, GMet observations indicate stronger positive trends in monthly total SD across several stations and climatic zones, whereas SARAH-3 trends are comparatively weaker and spatially smoother. However, these differences should be interpreted cautiously because valid temporal coverage differs between stations and between the two datasets after quality control filtering, and potential inhomogeneities in the surface observations cannot be fully excluded. Consequently, part of the observed trend differences may arise from differences in temporal sampling and data coverage rather than solely from physical inconsistencies between the datasets. The relatively weak trends in the zonal mean bias series suggest that SARAH-3 remains comparatively stable relative to the surface observations despite the differing absolute trends identified in the station-level analyses.

A key contribution of this study is the explicit quantification of the coupling between SD bias and AOD. Strong positive correlations during DJF, together with regression slopes linking SARAH–GMet sunshine bias to MERRA–SARAH AOD bias, demonstrate that aerosol absorption and scattering exert a first-order control on SD retrieval errors. In contrast, the weak relationships observed during JJA highlight the dominance of deep convective cloud systems, where cloud optical thickness overwhelms aerosol effects and reduces the sensitivity of SARAH-3 retrievals to aerosol variability. Frequency distribution analysis further reveals that SARAH-3 systematically under-detects very low sunshine conditions, particularly over the Coastal Savannah during JJA. Days with near-zero SD in GMet observations are frequently assigned to values larger than GMet values by SARAH-3, indicating a limitation in resolving persistent low-irradiance regimes associated with marine stratus, shallow convection, and broken cloud fields. This finding has important implications for applications requiring accurate representation of cloudy days, such as solar energy yield estimation, agricultural modelling, and hydrological studies.

Taken together, the results demonstrate that SARAH-3 provides a robust and spatially consistent representation of sunshine duration climatology over Ghana but exhibits seasonally dependent biases.

Future developments of the SARAH product could benefit from MERRA-2 AOD to better represent aerosol attenuation effects under clear-sky and dry-season conditions. Given the demonstrated coupling between AOD bias and sunshine duration bias, improved aerosol characterization may enhance retrieval performance over West Africa, especially during the Harmattan season.

5 References

Asilevi, P. J., Dzidzorm, E. N., Boakye, P., & Quansah, E. (2025). Nitrogen dioxide (NO2) Meteorology and predictability for air quality management using TROPOMI. Npj Clean Air, 1(1), 3
https://doi.org/10.1038/s44407-024-00003-4

Asilevi, P. J., Quansah, E., Amekudzi, L. K., Annor, T., & Klutse, N. A. B. (2019). Modeling the spatial distribution of Global Solar Radiation (GSR) over Ghana using the Ångström-Prescott sunshine duration model. Scientific African, 4, e00094
https://doi.org/10.1016/j.sciaf.2019.e00094

Asilevi Junior, P., Opoku, N. K., Martey, F., Setsoafia, E., Ahafianyo, F., Quansah, E., ... & Padi, M. (2022). Development of High Resolution Cloud Cover Climatology Databank Using Merged Manual and Satellite Datasets over Ghana, West Africa. Atmosphere-Ocean, 60(5), 566-579
https://doi.org/10.1080/07055900.2022.2072266

Bellouin, N., Quaas, J., Gryspeerdt, E., Kinne, S., Stier, P., Watson-Parris, D., ... & Stevens, B. (2020). Bounding global aerosol radiative forcing of climate change. Reviews of Geophysics, 58(1), e2019RG000660
https://doi.org/10.1029/2019RG000660

Clauzel, L., Anquetin, S., Lavaysse, C., Bergametti, G., Bouet, C., Siour, G., ... & Thomas, J. (2025). Solar radiation estimation in West Africa: impact of dust conditions during the 2021 dry season. Atmospheric Chemistry and Physics, 25(2), 997-1021
https://doi.org/10.5194/acp-25-997-2025

Dogbey, F., Asilevi, P. J., Dzrobi, J. F., Koffi, H. A., & Klutse, N. A. B. (2022). Modelling cloud cover climatology over tropical climates in Ghana. Atmosphere, 13(8), 1265
https://doi.org/10.3390/atmos13081265

Hollmann, R., Mueller, R. W., & Gratzki, A. (2006). CM-SAF surface radiation budget: First results with AVHRR data. Advances in Space Research, 37(12), 2166-2171.
https://doi.org/10.1016/j.asr.2005.10.044

Karlsson, K. G., Anttila, K., Trentmann, J., Stengel, M., Fokke Meirink, J., Devasthale, A., ... & Hollmann, R. (2017). CLARA-A2: the second edition of the CM SAF cloud and radiation data record from 34 years of global AVHRR data. Atmospheric Chemistry and Physics, 17(9), 5809-5828.

https://doi.org/10.5194/acp-17-5809-2017

Knippertz, P., Fink, A. H., Deroubaix, A., Morris, E., Tocquer, F., Evans, M. J., ... & Schlueter, A. (2017). A meteorological and chemical overview of the DACCIWA field campaign in West Africa in June–July 2016. Atmospheric Chemistry and Physics, 17(17), 10893-10918
https://doi.org/10.5194/acp-17-10893-2017

Kothe, S., Pfeifroth, U., Cremer, R., Trentmann, J., & Hollmann, R. (2017). A satellite-based sunshine duration climate data record for Europe and Africa. Remote Sensing, 9(5), 429
https://doi.org/10.3390/rs9050429

Manara, V., Beltrano, M. C., Brunetti, M., Maugeri, M., Sanchez-Lorenzo, A., Simolo, C., & Sorrenti, S. (2015). Sunshine duration variability and trends in Italy from homogenized instrumental time series (1936–2013). Journal of Geophysical Research: Atmospheres, 120(9), 3622-3641
https://doi.org/10.1002/2014JD022560

Pfeifroth, U., Drücke, J., Kothe, S., Trentmann, J., Schröder, M., & Hollmann, R. (2024). SARAH-3–satellite-based climate data records of surface solar radiation. Earth System Science Data, 16(11), 5243-5265
https://doi.org/10.5194/essd-16-5243-2024

Pfeifroth, U., Kothe, S., Drücke, J., Trentmann, J., Schröder, M., Selbach, N., & Hollmann, R. (2023). Surface Radiation Data Set-Heliosat (SARAH)-Edition 3, Satellite Application Facility on Climate Monitoring.
https://doi.org/10.5676/EUM_SAF_CM/SARAH/V003

Pfeifroth, U., Sanchez-Lorenzo, A., Manara, V., Trentmann, J., & Hollmann, R. (2018). Trends and variability of surface solar radiation in Europe based on surface-and satellite-based data records. Journal of Geophysical Research: Atmospheres, 123(3), 1735-1754.
https://doi.org/10.1002/2017JD027418

Pinker, R. T., Liu, H., Osborne, S. R., & Akoshile, C. (2010). Radiative effects of aerosols in sub-Sahel Africa: Dust and biomass burning. Journal of Geophysical Research: Atmospheres, 115(D15)
https://doi.org/10.1029/2009JD013335

Randles, C. A., Da Silva, A. M., Buchard, V., Colarco, P. R., Darmenov, A., Govindaraju, R., ... & Flynn, C. J. (2017). The MERRA-2 aerosol reanalysis, 1980 onward. Part I: System description and data assimilation evaluation. Journal of climate, 30(17), 6823-6850
https://doi.org/10.1175/JCLI-D-16-0609.1

Sánchez-Romero, A., González, J. A., Calbó, J., & Sánchez-Lorenzo, A. (2015). Using digital image processing to characterize the Campbell–Stokes sunshine recorder and to derive high-temporal resolution direct solar irradiance. Atmospheric Measurement Techniques, 8(1), 183-194
https://doi.org/10.5194/amt-8-183-2015

Sawadogo, W., Neya, T., Semde, I., Korahiré, J. A., Combasséré, A., Traoré, D. E., ... & Kunstmann, H. (2024). Potential impacts of climate change on the sudan-sahel region in West Africa–Insights from Burkina Faso. Environmental Challenges, 15, 100860
https://doi.org/10.1016/j.envc.2024.100860

Wild, M. (2009). Global dimming and brightening: A review. Journal of Geophysical Research: Atmospheres, 114(D10)
https://doi.org/10.1029/2008JD011470

Wild, M. (2016). Decadal changes in radiative fluxes at land and ocean surfaces and their relevance for global warming. Wiley Interdisciplinary Reviews: Climate Change, 7(1), 91-107
https://doi.org/10.1002/wcc.372

Wild, M., Folini, D., Schär, C., Loeb, N., Dutton, E. G., & König-Langlo, G. (2013). The global energy balance from a surface perspective. Climate dynamics, 40(11), 3107-3134
https://doi.org/10.1007/s00382-012-1569-8

WM Organization. (2008). WMO Guide to Meteorological Instruments and Methods of Observation

6 Glossary – List of Acronyms in alphabetical order

AC SAF - Satellite Application Facility on Atmospheric Composition Monitoring

AOD - Aerosol Optical Depth

CDR - Climate Data Record

CM SAF - Satellite Application Facility on Climate Monitoring

CRS - Climate Reference Station

DJF - December–January–February (boreal winter season)

DWD - Deutscher Wetterdienst (German Meteorological Service)

EO - Earth Observation

EUMETSAT – European Organisation for the Exploitation of Meteorological Satellites

GHA - Ghana (used in shapefile and spatial mapping context)

GMet - Ghana Meteorological Agency

h/day - Hours per day

h/decade (h/dec) - Hours per decade

h/month - Hours per month

JJA - June–July–August (boreal summer season)

Kendall τ - Kendall rank correlation coefficient

MAM - March–April–May (boreal spring season)

MERRA-2 - Modern-Era Retrospective analysis for Research and Applications, Version 2

OLS - Ordinary Least Squares

r - Pearson correlation coefficient

RMSE - Root Mean Square Error

SARAH - Surface Solar Radiation Data Set – Heliosat

SD - Sunshine Duration

SON - September–October–November (boreal autumn season)

τ (tau) - Kendall's tau rank correlation coefficient

WMO - World Meteorological Organization

7 Appendix

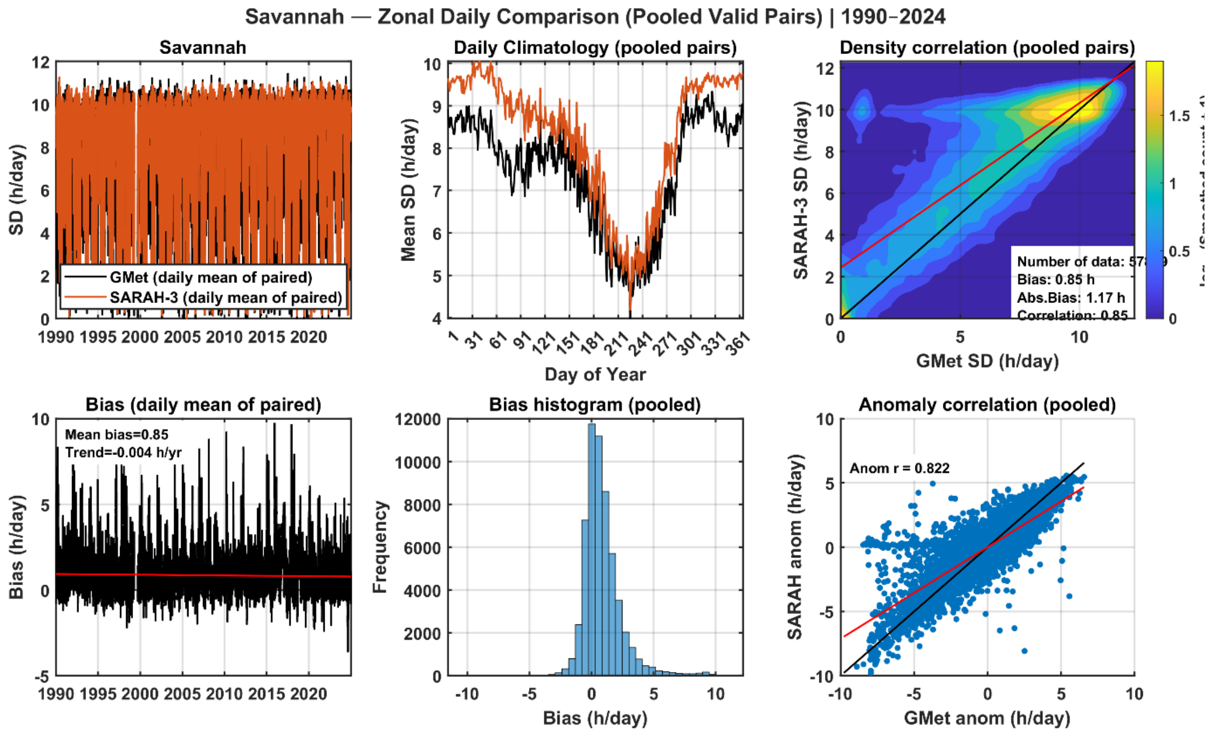

Figure 7-1: Comparison of daily climatology over the Savannah zone.

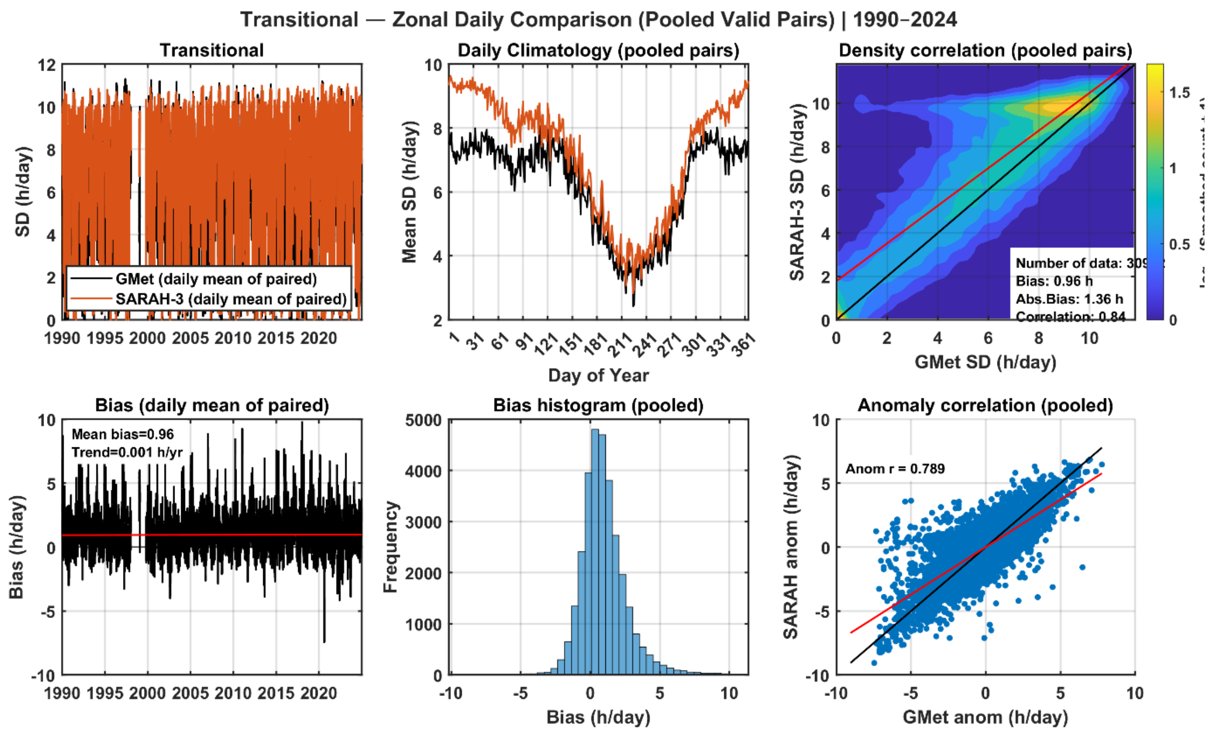

Figure 7-2: Comparison of daily climatology over the Transition zone.

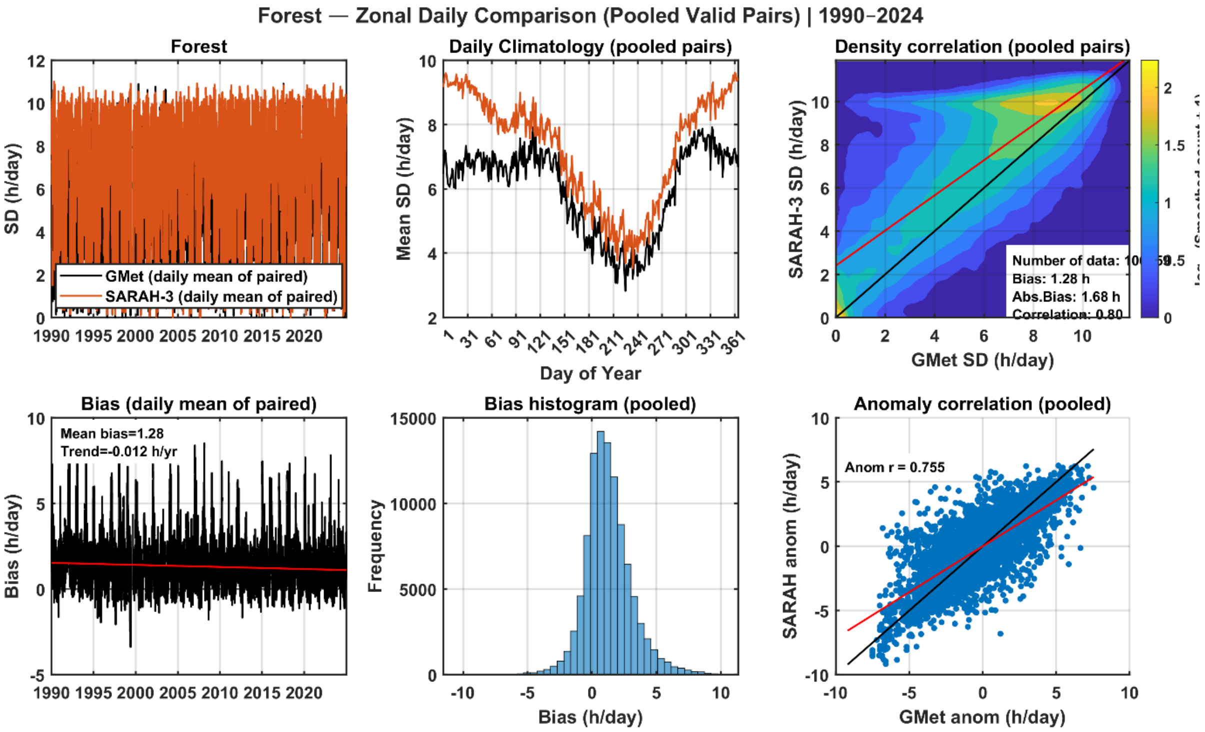

Figure 7-3: Comparison of daily climatology over the Forest zone.

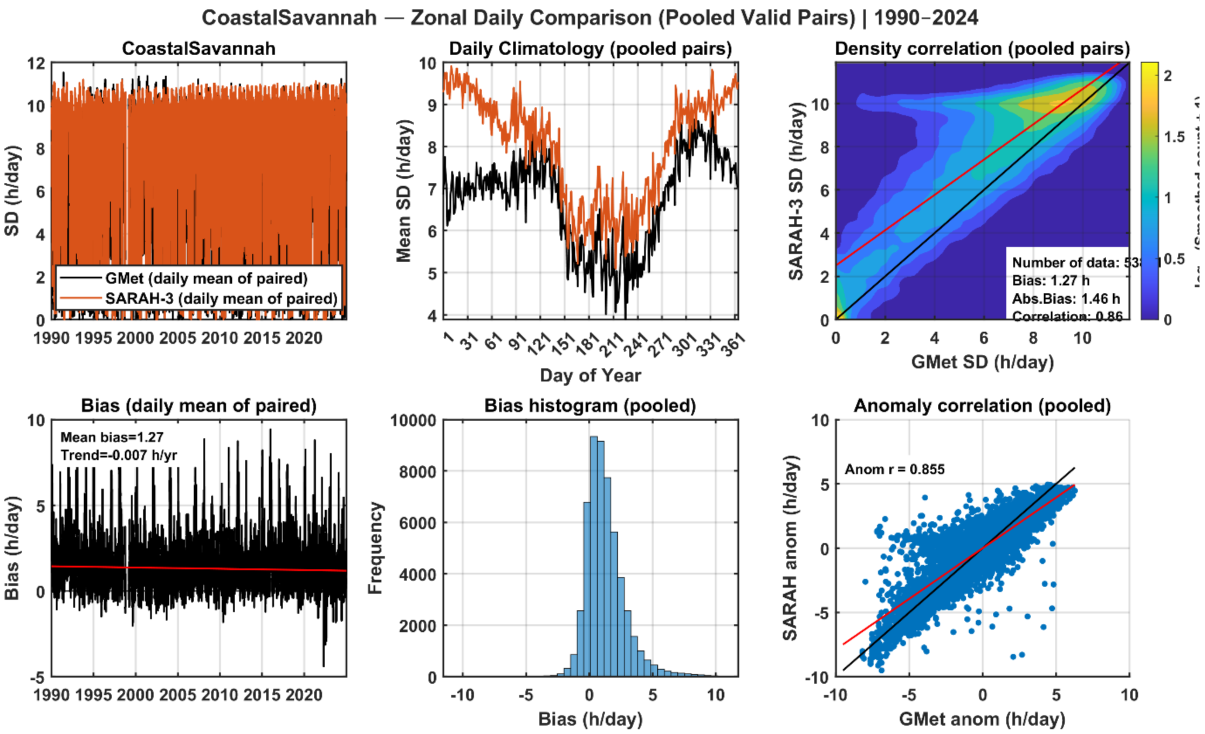

Figure 7-4: Comparison of daily climatology over the Coastal zone.

Table 7-1: A station by station comparison of seasonal mean SARAH-3 and GMet SD bias (h/ day)

Station	DJF Bias	MAM Bias	JJA Bias	SON Bias
Wa	0.79	0.89	0.45	0.62
Navrongo	0.86	1.31	0.54	0.80
Bole	1.26	0.94	0.58	0.87
Tamale	1.22	1.22	0.62	0.71
Yendi	1.32	0.88	0.22	0.69
Wenchi	1.41	0.68	0.15	0.33
Sunyani	2.14	1.42	0.82	1.11
Kete Krachi	1.73	0.90	0.49	0.54
Kumasi	2.60	1.64	1.11	1.29
Sefwi Bekwai	2.58	1.27	0.84	1.28
Akim Oda	2.81	1.38	0.74	0.94
Abetifi	1.35	0.45	0.00	0.32
Koforidua	2.21	1.34	1.56	1.33
Ho	1.83	0.88	0.63	0.58
Akuse	2.37	1.41	1.21	1.00
Axim	2.07	0.59	0.12	0.46
Takoradi	2.17	1.21	1.40	1.24
Saltpond	1.87	0.91	1.14	0.98
Accra	2.25	1.21	1.19	0.97
Tema	1.92	0.94	1.00	1.01
Ada	2.00	0.99	0.99	0.86
Akatsi	2.18	1.29	0.91	0.93

Table 7-2: Comparison of all coastal cases within the study period where GMet SD was below 1 h day^{-1} but SARAH-3 reported higher SD values

Date	Station	Sunshine Duration (SD, h/ day)		
		Gmet	SARAH-3	Bias
6/26/1990 0:00	Akatsi	0.9	4.38	3.48
7/21/1990 0:00	Akatsi	0.4	5.08	4.68
8/2/1990 0:00	Accra	0.6	4.28	3.68
8/28/1990 0:00	Saltpond	0.4	4.4	4
6/10/1991 0:00	Saltpond	0.7	4.53	3.83
6/18/1992 0:00	Akatsi	0.7	4.13	3.43
7/2/1993 0:00	Akatsi	0.8	5.04	4.24
7/29/1994 0:00	Saltpond	0.6	4.1	3.5
8/17/1995 0:00	Accra	0.9	4.61	3.71
8/16/1997 0:00	Accra	0.9	4.07	3.17

7/12/1999 0:00	Accra	0.5	4.97	4.47
8/6/2001 0:00	Saltpond	0.9	4.19	3.29
6/21/2004 0:00	Tema	0.5	4.46	3.96
7/18/2004 0:00	Saltpond	0.2	4.94	4.74
8/14/2005 0:00	Accra	0.3	4	3.7
8/19/2006 0:00	Accra	0.5	4.32	3.82
6/16/2009 0:00	Ada	0.5	4.31	3.81
7/18/2009 0:00	Akatsi	0	4.1	4.1
8/29/2009 0:00	Ada	0.6	5.67	5.07
7/28/2011 0:00	Accra	0.9	4.16	3.26
8/13/2011 0:00	Tema	0.7	4.34	3.64
8/23/2011 0:00	Accra	0.6	4.48	3.88
7/24/2012 0:00	Accra	0.5	4.22	3.72
7/29/2012 0:00	Tema	0.8	4.18	3.38
8/11/2012 0:00	Saltpond	0.6	5	4.4
8/22/2013 0:00	Saltpond	0.4	4.31	3.91
8/31/2013 0:00	Ada	0.8	4.42	3.62
8/31/2013 0:00	Tema	0.4	4.66	4.26
8/14/2014 0:00	Saltpond	0.2	5.83	5.63
7/4/2015 0:00	Saltpond	0.7	5.21	4.51
7/14/2016 0:00	Akatsi	0.7	5.45	4.75
7/25/2016 0:00	Saltpond	0.6	4.08	3.48
8/8/2016 0:00	Ada	0.8	4.05	3.25
8/18/2016 0:00	Accra	0.9	4.36	3.46
8/19/2016 0:00	Ada	0.8	6	5.2
8/22/2016 0:00	Saltpond	0.1	4.23	4.13
6/13/2017 0:00	Accra	0.8	4.38	3.58
6/13/2017 0:00	Saltpond	0.9	4.94	4.04
8/7/2018 0:00	Saltpond	0.5	5.57	5.07
8/18/2018 0:00	Saltpond	0.6	5.84	5.24
8/21/2018 0:00	Saltpond	0.5	4.9	4.4
8/28/2018 0:00	Saltpond	0.5	4.72	4.22
8/31/2018 0:00	Saltpond	0.3	4.56	4.26
7/12/2022 0:00	Tema	0.1	4.71	4.61
7/25/2022 0:00	Tema	0.6	4.99	4.39
8/21/2023 0:00	Saltpond	0.6	4.62	4.02
6/3/2024 0:00	Saltpond	0.8	5.98	5.18
8/31/2024 0:00	Accra	0.8	4.22	3.42

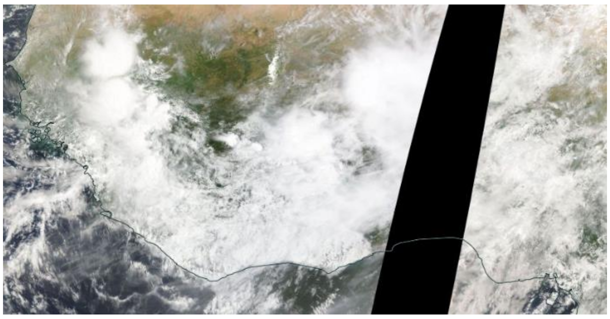

8/31/2024

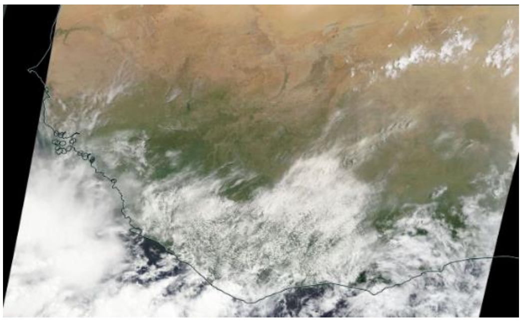

6/13/2017

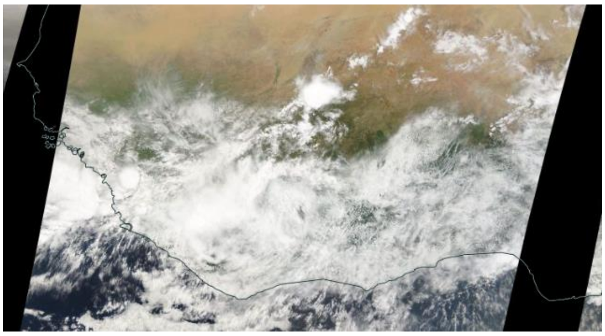

7/18/2009 0:00

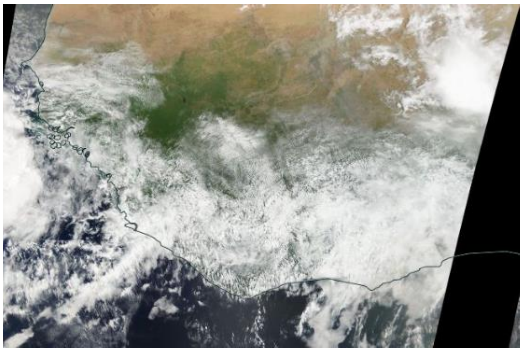

7/24/2012

Figure 7-5: Sample satellite images confirming SD <1 hour as recorded by GMet. Photo derived from https://worldview.earthdata.nasa.gov/.